

# ESTIMATING WITHIN-FIELD VARIATIONS IN SOIL PROPERTIES FROM AIRBORNE HYPERSPECTRAL IMAGES

**Suk Young Hong**, Visiting Research Associate  
**Kenneth A. Sudduth**, Agricultural Engineer  
**Newell R. Kitchen**, Soil Scientist  
**Scott T. Drummond**, Computer Specialist  
Cropping Systems and Water Quality Research Unit  
USDA-ARS  
Columbia, MO 65211  
HongS@missouri.edu  
SudduthK@missouri.edu  
KitchenN@missouri.edu  
DrummondS@missouri.edu

**Harlan L. Palm**, Research Assistant Professor  
**William J. Wiebold**, Associate Professor  
University of Missouri  
Columbia, MO 65211  
PalmH@missouri.edu  
WieboldW@missouri.edu

## ABSTRACT

The ability of hyperspectral image (HSI) data to provide estimates of soil electrical conductivity ( $EC_a$ ) and soil fertility levels without requiring extensive field data collection was investigated. The relationships between HSI spectral reflectance signatures and soil properties were analyzed to evaluate the usefulness of HSI for quantifying within-field spatial variability. Bare soil images were acquired using a prism grating pushbroom scanner in April 2000 and May 2001 for a central Missouri experimental field in a minimum-tillage corn-soybean rotation. Data were converted to reflectance using chemically-treated reference tarps with eight known reflectance levels. Geometric distortions of the pushbroom sensor images were corrected with a rubber sheeting transformation. A 5 m pixel size was selected by analysis of short-range variations in five sub-field areas. Statistical analyses, including simple correlation, multiple regression (MR), and principal component analysis (PCA) were used to relate HSI data and derived Landsat-like bands to field-measured soil properties. The blue wavelengths of the HSI and Landsat-like images showed the highest correlation with  $EC_a$  and soil chemical properties. With the exception of pH and P, the soil fertility data were negatively correlated to the HSI reflectance data. The highest correlations to the HSI bands were found for Mg and CEC. Stepwise multiple linear regression (SMLR) models using the full HSI dataset included too many variables, which increased the danger of overfitting. MR models using Landsat-like bands may be more practical than using SMLR models for mapping soil properties. Analysis of principal components showed that PC 2 and PC 4 explained soil variability well for CEC, Mg, OM, K, and pH. Both approaches to data volume reduction, creating Landsat-like bands and PCA, showed potential for developing relationships with soil properties. HSI analysis appears promising for quantifying soil property variability.

## INTRODUCTION

Precision agriculture, or site-specific crop management (SSCM), is an information-based management-intensive approach to farming. Instead of managing a field as a whole, the philosophy of precision agriculture is to manage individual areas within a field. Accounting for soil variability is a critical need for SSCM. Traditionally, quantification and mapping of soil properties have been done through relatively coarse grid soil sampling and statistical interpolation.

Soil electrical conductivity ( $EC_a$ ) measurements collected by ground-based sensors have been used to describe within-field variability in soil physical and chemical properties (Sudduth *et al.*, 2002), and have also been correlated with crop yield variations (Kitchen *et al.*, 1999). In traditional precision agriculture applications, soil fertility

## ESTIMATING WITHIN-FIELD VARIATIONS IN SOIL PROPERTIES FROM AIRBORNE HYPERSPECTRAL IMAGES

variability has been characterized by grid soil sampling and laboratory analysis. These procedures are costly, time-consuming, and provide relatively low resolution data. Methods that could estimate these soil properties more efficiently would be useful. Widespread implementation of precision agriculture will require methods for more efficiently and economically characterizing variations in soil properties and other factors that affect crop yields.

Image-based remote sensing (RS) is an efficient way to detect spatial differences in crop and soil conditions within a field. The recent convergence of technological advances in geographic information systems (GIS), global positioning systems (GPS), and automatic control of farm machinery through variable rate technology (VRT) have provided an ideal framework for utilizing RS for farm management (Moran, 2000). Remote sensing data are also useful in helping to define management units. Remote sensing offers the potential for identifying fine scale spatial patterns in soil properties across a field, and optimizing soil sampling strategies to quantify those patterns (Mulla *et al.*, 2000).

Recently, a variety of aircraft and satellite based RS data such as photographs, videographs, hyperspectral and multispectral images have become available for use in agricultural applications. Imaging spectrometry (also known as hyperspectral sensing), is defined as the simultaneous acquisition of images in many relatively narrow, contiguous and/or non-contiguous spectral bands throughout the ultraviolet, visible and infrared portions of the spectrum (Jensen, 2000). The value of an imaging spectrometer lies in its ability to provide a high-resolution reflectance spectrum for each picture element in the image. The reflectance spectrum in the region from 400-2500 nm may be used to identify a large range of surface cover materials that cannot be identified with broadband, low-spectral-resolution imaging systems such as the Landsat MSS, TM, or SPOT (Goetz *et al.*, 1985).

Airborne pushbroom scanning provides an effective method for hyperspectral imaging (HSI) with a low cost digital CCD camera (Mao, 2000). However, the data obtained with an aerial pushbroom HSI system suffers from geometric distortions. Some of the distortions are caused by aircraft attitude changes during image scanning. When the aircraft attitude changes, the scanner is presented with an off-nadir scene, causing distortion. This problem is especially severe in the in-track direction due to roll of the aircraft. These distortions must be corrected before the image data can be geo-referenced and used for field pattern identification (Yao *et al.*, 2001).

The objective of this study was to explore the relationships between airborne HSI spectral reflectance signatures and soil properties, and to evaluate the usefulness of HSI for quantifying within-field spatial variability. In particular, we were interested in the ability of HSI data to provide estimates of soil EC<sub>a</sub> and soil fertility levels without requiring extensive field data collection.

## **GROUND DATA COLLECTION AND PROCESSING**

Data were collected on a research field (Field 1, 35 ha) located near Centralia, Missouri (92.12 E – 39.97 N). Field 1 is in a corn-soybean rotation, and data were obtained for one soybean (2000) and one corn (2001) crop year. The soils found at these sites are claypan soils of the Mexico-Putnam association (fine, smectitic, mesic aeris Vertic Aqualfs). Mexico-Putnam soils formed in moderately-fine textured loess over a fine textured pedisegment. Surface textures range from a silt loam to a silty clay loam. The subsoil claypan horizon(s) are silty clay loam, silty clay or clay, and commonly contain as much as 50 to 60% montmorillonitic clay. Within the study field, topsoil depth above the claypan ranged from less than 10 cm to greater than 100 cm. Because of the high-clay subsurface horizons, topsoil depth above the claypan is often correlated to spatial variations in crop productivity (Kitchen *et al.*, 1999).

Ground measurements used in this analysis included soil EC<sub>a</sub> and soil chemical properties. Soil EC<sub>a</sub> was measured for each field in the fall of 1999 using two commercial sensor systems, the Geonics EM38 and the Veris 3100. The EM38 operates on the principle of electromagnetic induction and, as operated in the vertical dipole mode, provides an effective measurement depth of approximately 1.5 m. The EM38 was used in a GPS-enabled mobile system described by Sudduth *et al.* (2001) to collect data every 1 second on measurement transects spaced 10 m apart. The Veris 3100 is a complete commercial system that measures EC<sub>a</sub> through coulter electrodes that penetrate the ground surface. This device provides both a shallow and deep reading, with effective measurement depths of approximately 0.3 m and 1.0 m. Data was collected every 1 s on a 10 m transect spacing. At the operating speeds used, this time interval corresponded to 4 to 6 m spacing between sample points. Soil EC<sub>a</sub> data were analyzed using geostatistics, and interpolated by block kriging to a 5 m cell size using appropriate semivariogram models. In previous research, we have found these two sensors to provide similar, but not identical mapped EC<sub>a</sub> information on claypan-soil fields (Sudduth *et al.*, 1998). Both the EM38 and Veris deep readings have been shown to be reliable estimators of topsoil depth in claypan soils (Sudduth *et al.*, 1998; Kitchen *et al.*, 1999; Sudduth *et al.*, 2001).

### **ESTIMATING WITHIN-FIELD VARIATIONS IN SOIL PROPERTIES FROM AIRBORNE HYPERSPECTRAL IMAGES**

The field was sampled on a 33 m grid to a 15 cm depth in the spring of 2001 and analyzed for P (Bray 1 extractable), K, Ca, Mg (ammonium acetate extractable), CEC (sum of bases), organic matter (OM; wet oxidation), and salt pH, all using standard University of Missouri procedures (Brown and Rodriguez, 1983). Soil sampling point coordinates were later used to extract coincident spectral signatures obtained from the HSI data.

## **HYPERSPECTRAL IMAGE PROCESSING AND DATA ANALYSIS**

Airborne images of bare soil were taken in April 2000 and May 2001. The aerial HSI system used in this study was a pushbroom prism-grating scanner (RDACSH3; Real Time Digital Airborne Camera System H3) operated by Spectral Visions Midwest (Mao, 2000). Images included 120 bands ranging from 471-828 nm (3 nm interval) with a spatial resolution of 1 m and 1.5 nm Full Width at Half Maximum (FWHM). Pushbroom scanning is a widely used method for airborne HSI in which an airborne imaging sensor acquires one image line at a time while the aircraft provides a mobile platform to carry the sensor across the target area.

Geometric distortion was observed in the images, probably due to aircraft attitude change during image acquisition. In general, such geometric distortion should be corrected by the acquisition system since flight information can be used to correct image distortion. We applied a rubber sheeting model using piecewise polynomials for image rectification rather than a linear polynomial transformation. Foghani (2000) reported that a more precise image could be obtained by using a rubber sheeting procedure, compared to polynomial adjustment or an orthophotography algorithm. The Field 1 boundary had been very accurately surveyed, and that vector data was used along with a resolution-merged IKONOS image with a spatial resolution of 1 m taken on August 4, 2000. The IKONOS image was registered and matched with the field boundary and used as a reference image for georeferencing airborne imagery. Rubber sheeting models are not recommended for rectification of areas outside of the field of interest because of geometric uncertainty, and should be used only when the geometric distortion is severe, ground control points are abundant, and no other geometric model is applicable (ERDAS, 1997).

For radiometric calibration, chemically-treated reference tarps with eight known reflectance levels from 2% to 88%, (a range wide enough to represent all field surface reflection conditions) were used. The tarps were placed adjacent to Field 1 during flights and reflectance values were retrieved from the images by regression models of reflectance against the 120 spectral bands.

While the HSI data had a spatial resolution of 1 m, this level of resolution was not necessarily desirable if the image contained significant random noise. The amount of random noise throughout the wavelengths was determined by checking spatial profiles of the images, since soil properties are continuous phenomena in nature. Five representative areas in Field 1 were used to determine the optimum pixel size for data analysis. Subset images were re-sampled at various levels of image aggregation ranging from a 1 m to a 10 m pixel size. Standard deviations of each subset area revealed that most short-range variations were removed at a 5 m spatial resolution. Image degradation was applied to provide 5 m images for further data analysis.

Principal component analysis (PCA) was completed on each image and used as a data set for further statistical analysis. PCA is a procedure for transforming a set of correlated variables into a new set of uncorrelated variables, termed principal components (PCs). This transformation is a rotation of the original axes to new orientations that are orthogonal to each other, thus there are no correlations among the transformed variables. Another property of PCA is that the majority of the information contained in a large set of highly correlated variables (wavelengths, in this case) can be represented with a much smaller number of PCs. The first five PCs of each image were used for data analysis. Using the GPS coordinates for soil EC<sub>a</sub> and soil chemical properties, pixel values of coincident points on the imagery were extracted, and PCs calculated.

In addition to PCA, standard correlation, multiple regression (MR), and stepwise multiple linear regression (SMLR) analyses were carried out to determine the relationships between HSI image signatures and ground-collected soil data. Soil EC<sub>a</sub> and soil chemical property data were regressed against HSI data, 4 Landsat-like bands, and the 5 PCs of the Field 1 images taken in both years. Soil EC<sub>a</sub> and fertility maps derived from regression models and PCs were compared with ground sensed data.

## **SOIL PROPERTIES AND HYPERSPECTRAL SIGNATURES**

Soil reflectance is a function of the soil's chemical and physical composition (Bowers and Hanks, 1965). Optical properties of soils are related first to their mineral composition, since soils result from the transformation of

### **ESTIMATING WITHIN-FIELD VARIATIONS IN SOIL PROPERTIES FROM AIRBORNE HYPERSPECTRAL IMAGES**

weathering products of rocks. A soil reflectance is generally low but increases monotonically with wavelength through the visible and near-infrared regions of the electromagnetic spectrum (Obukhov and Orlov, 1964; Orlov, 1966). Soil color is a useful indicator of soil type and soil properties (Karmanov and Rozhkov, 1972). The spectral reflectance of soil is also influenced by moisture content, organic matter, particle size, iron oxide, mineral composition, soluble salts, parent materials, and other factors (Baumgardner *et al.*, 1985; Sudduth and Hummel, 1991).

Since hyperspectral data are often highly redundant, data compression or reduction is an important pre-processing step. To compare the relative usefulness of the HSI data, we averaged reflectance values of the HSI data spectrally to make Landsat-like bands. Two data sets, the first consisting of the 120 HSI data layers and the second consisting of 4 Landsat-like data layers, were used for statistical analysis in this study.

When the two bare soil images taken in 2000 and 2001 were visually compared, the 2001 image was generally darker than the 2000 image (Figure 1). The 2001 image showed much more contrast in the poorly drained areas of the field (i.e., the water drainage channel) and between the foot slope and side slope areas of the northern part of the field. Climatological conditions may help to explain these observations. In 2000, only 4 mm of precipitation was observed during the 2 weeks prior to image acquisition. In 2001, a total of 60 mm was recorded in the 2 weeks prior to the flight. Since flow accumulation, redistribution, and infiltration would have been expected to differ considerably across landscape positions within this field, surface soil moisture variations would have been significantly larger in 2001 than in 2000.

Figure 2 more clearly illustrates this point. Soil lines for both bare soil images on Field 1 were plotted into red-NIR space. For a given soil, the red ( $r_g$ ) and near-infrared ( $nir_g$ ) reflectances are related by the equation of the soil line:  $nir_g = a \cdot r_g + b$  (Baret and Guyot, 1991). The parameters  $a$  and  $b$  vary slightly among soils (Huete *et al.*, 1984). Spectral reflectance of the wet (2001) soil was lower than that of the dry (2000) soil, narrower in terms of data range, and had a greater deviation from the trend line. Meanwhile dry soil had wider data range and a smaller deviation from the trend line. This tighter fit might allow for a better relationship between spectral signature and soil properties.

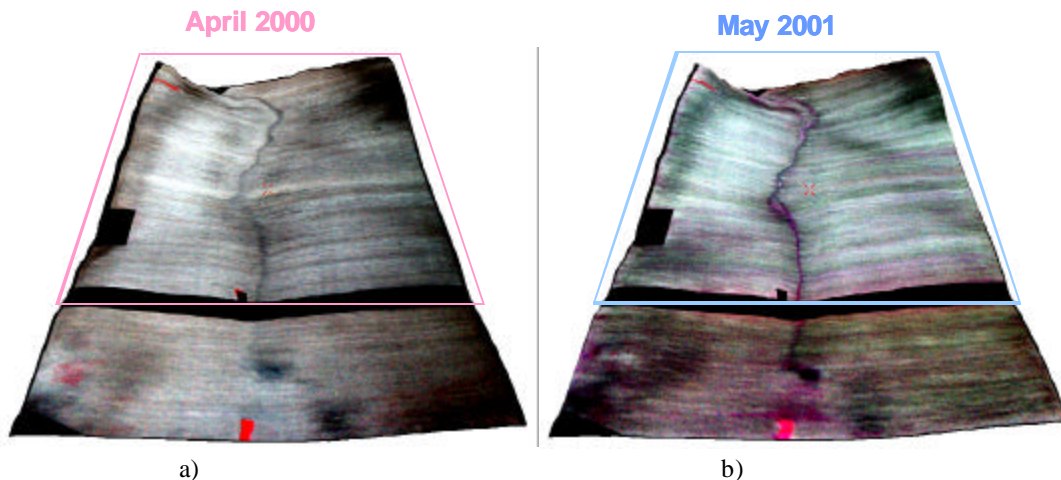


Figure 1. Two bare soil images of Field 1 taken in April 2000 (a) and May 2001 (b) for this study.

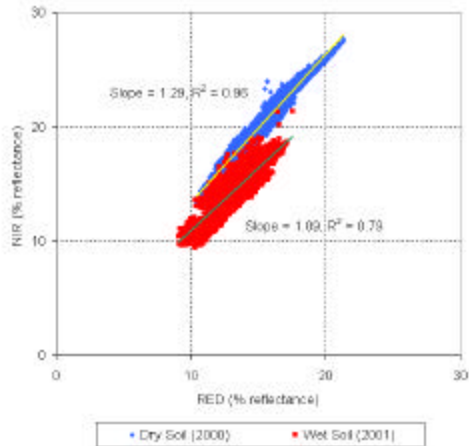


Figure 2. Soil lines, in red-NIR space, for Field 1 claypan soils, ranging from silt loam to silty clay

### Simple Correlation

To investigate the specific relationships present in this data, simple correlation analysis was completed and correlation coefficients ( $r$ ) were plotted against wavelength (Figures 3 and 4) to investigate the effective wavelength range for quantifying soil  $EC_a$  and chemical properties (pH, organic matter, P, Ca, Mg, K, and CEC). Soil  $EC_a$  had a strong negative correlation with all 120 HSI bands and 4 Landsat-like bands in the dry soil conditions of 2000 (Figure 3). The blue wavelengths showed the highest correlation with  $EC_a$ , with the correlation decreasing rapidly as the wavelength increased to around 560 nm. In the green and red wavelengths, correlation coefficients for  $EC_a$  were essentially constant. Of the  $EC_a$  data types, the EM38 reading was most highly correlated with the image data, while the Veris 3100 shallow (0-0.3 m) data showed the lowest correlations. A region of extremely noisy data was found in each correlation coefficient plot at around 740-750 nm (Figure 3). This is the location of an  $O_2$  and  $H_2O$  absorption band, where radiant energy is absorbed by these atmospheric constituents (Jensen, 2000). Correlation patterns in the NIR wavelengths showed some fluctuation, especially in the wet (2001) soil condition.

Soil chemical properties were related to blue, green, and red wavelengths in the visible region more strongly than they were to the near infrared wavelengths (Figure 4). This implied that the spectral reflectance signatures related to soil chemical properties were determined by soil color and thus, the factors influencing soil color also influenced soil chemical property variability. The patterns of the correlations for all cations show the same trends for both years. With the exception of pH and P, the soil fertility data were negatively correlated to the HSI reflectance data. Over the range of wavelengths the highest correlations to the HSI bands were found for Mg and CEC. For all soil properties, the highest correlations were generally found between 470 and 520 nm, in the blue bands of the visible region. Correlation with P was the most dissimilar between years. We feel this difference could be attributed to the fact that available P is an anion and will be independent of CEC/texture trends. Further, P is a managed soil property which varies over the field with uneven P fertilization. When correlation coefficients of Landsat-like bands were compared with those of the HSI bands, the results were quite similar (Figures 3 and 4). However, for the blue wavelengths only, the HSI bands seemed slightly more informative than the blue band of the Landsat-like image.

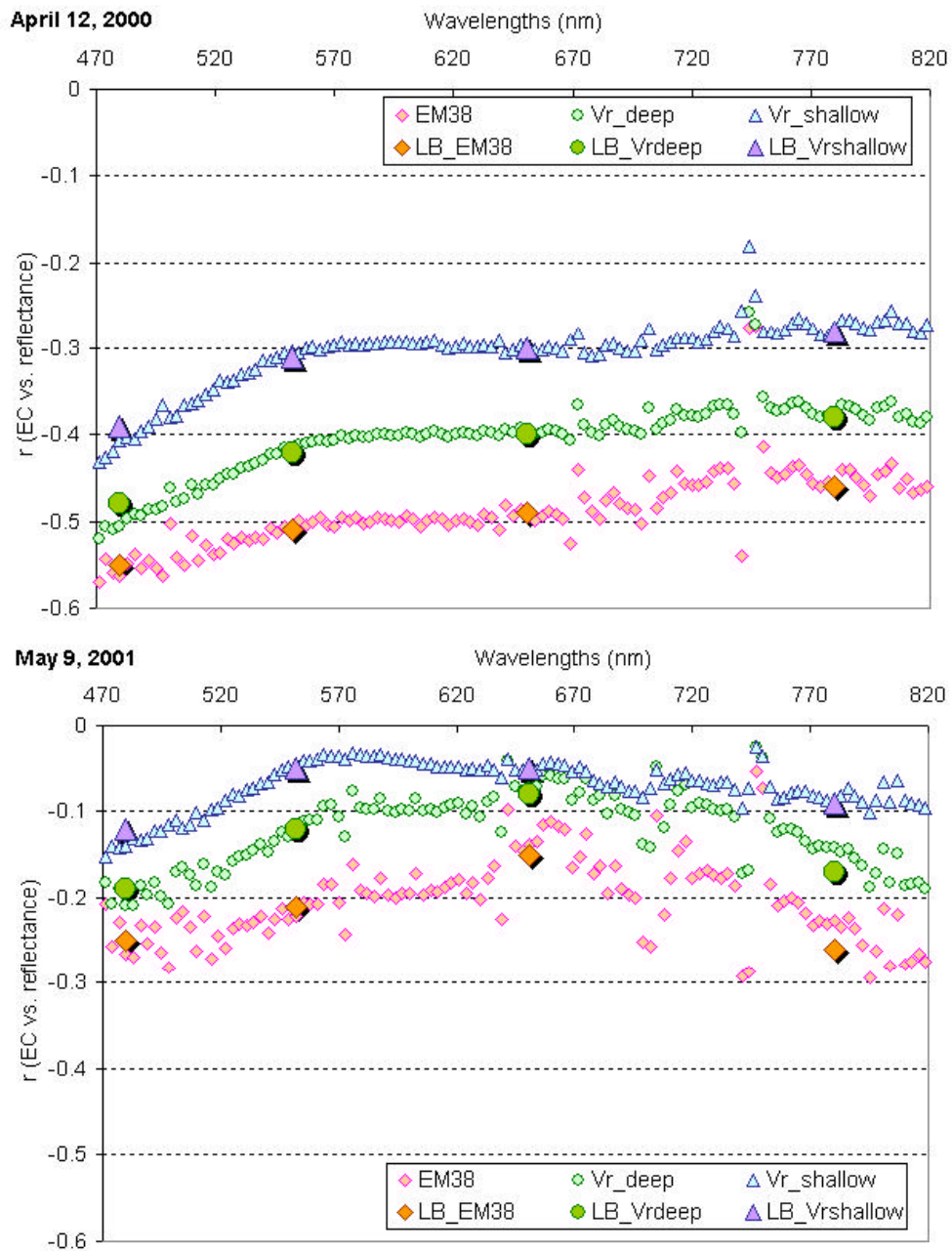


Figure 3. Correlations of 120 wavelengths and Landsat-like bands (LBs) to EM38 and Veris  $EC_a$  readings in 2000 (top) and 2001 (bottom).

**ESTIMATING WITHIN-FIELD VARIATIONS IN SOIL PROPERTIES FROM AIRBORNE  
HYPER SPECTRAL IMAGES**

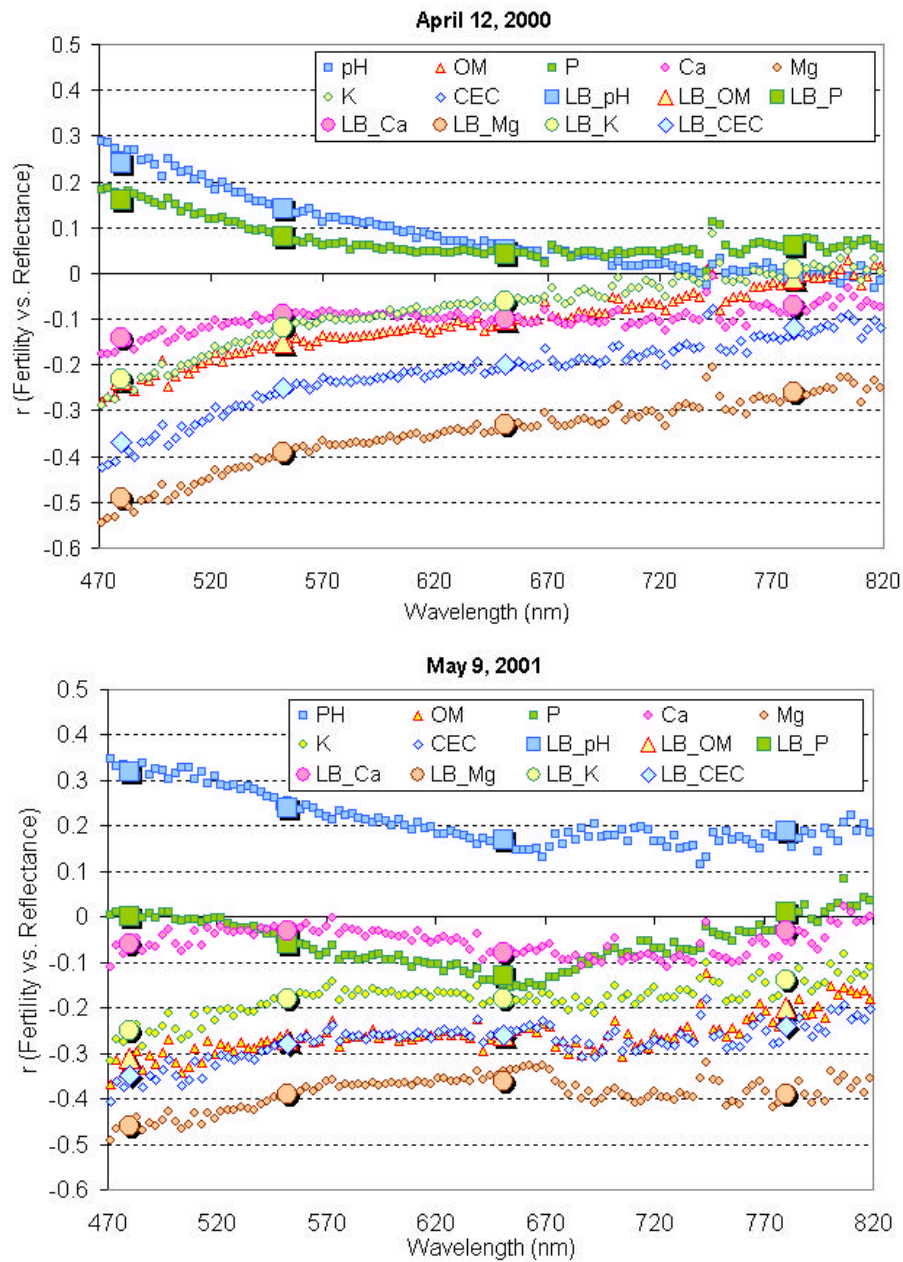


Figure 4. Correlations of 120 wavelengths and Landsat-like bands (LBs) to soil fertility by grid sampling in 2000 (top) and 2001(bottom).

## Multiple Regression

SMLR analysis was applied for estimating soil  $EC_a$  and soil chemical properties from HSI bands for both years. Model development continued until at least one parameter estimate was insignificant at the 0.15 level. The model results are shown in Table 1. The EM38  $EC_a$  data was best approximated using the HSI data. These data provided the most significant models both in 2000 ( $R^2 = 0.56$ ) and 2001 ( $R^2 = 0.43$ ). In terms of soil fertility, pH, Mg, and CEC were modeled from the HSI data with the highest  $R^2$  values of 0.68, 0.67, and 0.66, respectively. The SMLR procedure allowed many HSI bands to be included. Therefore, in addition to this "full" model, a conservative SMLR model, with  $R^2 \approx 95\%$  of the full model  $R^2$  was determined (Table 1). The intention of this model was to reduce the chance of overfitting the data, as compared to the full model. A similar approach worked well in a previous spectral data analysis (Sudduth and Hummel, 1991). On average, this reduced the number of wavelengths selected by over 50%, suggesting that little information was contained in those additional data (Table 1). Compared to soil  $EC_a$  models, the full models for soil fertility properties included fewer wavelengths and the reduction in number of wavelengths from the full to the conservative model was less (Table 1). This may have been due to the much smaller number of observations available for the soil fertility data ( $n=335$ ) as compared to the  $EC_a$  data ( $n=9588$ ).

Multiple regression (MR) of the 4 Landsat-like bands were performed for soil  $EC_a$  and soil fertility (Table 1). The  $R^2$  values of these MR models were always lower than those of the conservative SMLR models using 120 HSI bands for estimating soil properties. But SMLR models with a large number of independent variables included may be prone to overfit and provide poor predictions on a different data set. Therefore, MR models using Landsat-like bands may be more useful for mapping soil properties in practice.

Three  $EC_a$  maps derived from the 2000 image using these MR models are shown in Figure 5. Soil  $EC_a$  can be affected by a number of different soil properties including clay content, soil water content, varying depths of conductive soil layers, temperature, salinity, organic compounds, and metals (McNeill, 1992). On these claypan soil fields, soil  $EC_a$  is usually highest on eroded side-slopes. Here the claypan is often exposed, therefore the surface will have a much higher clay content than other landscape positions. The RS-estimated Veris shallow map nicely modeled the spatial pattern of the actual Veris data. As previously stated, the effective measurement depth of the Veris shallow system is about 0.3 m, while the other two readings measure to depths of 1 m or more. Since reflectance information comes from the soil surface, this better relationship with the shallow EC reading could be expected.

Soil fertility maps from grid sampling were compared with estimated soil fertility maps from the 4 Landsat-like bands of the 2000 image (Figure 6). High pH at the south end of the field (due to lime application several years prior) and the diagonal pattern of soil pH were obviously shown on the estimated pH map. CEC is derived from other cations, including Mg. The spatial pattern of CEC and Mg had similar trends and matched quite well with each estimated map from the Landsat-like bands. Soil organic matter was higher on eroded side-slopes than in other landscape positions, and Landsat-like band 1 was able to detect these high organic matter areas. We hypothesize that variation in soil clay content (primary factor) and organic matter (secondary factor) are the major soil conditions that control the relationship between spectral information and soil  $EC_a$ .

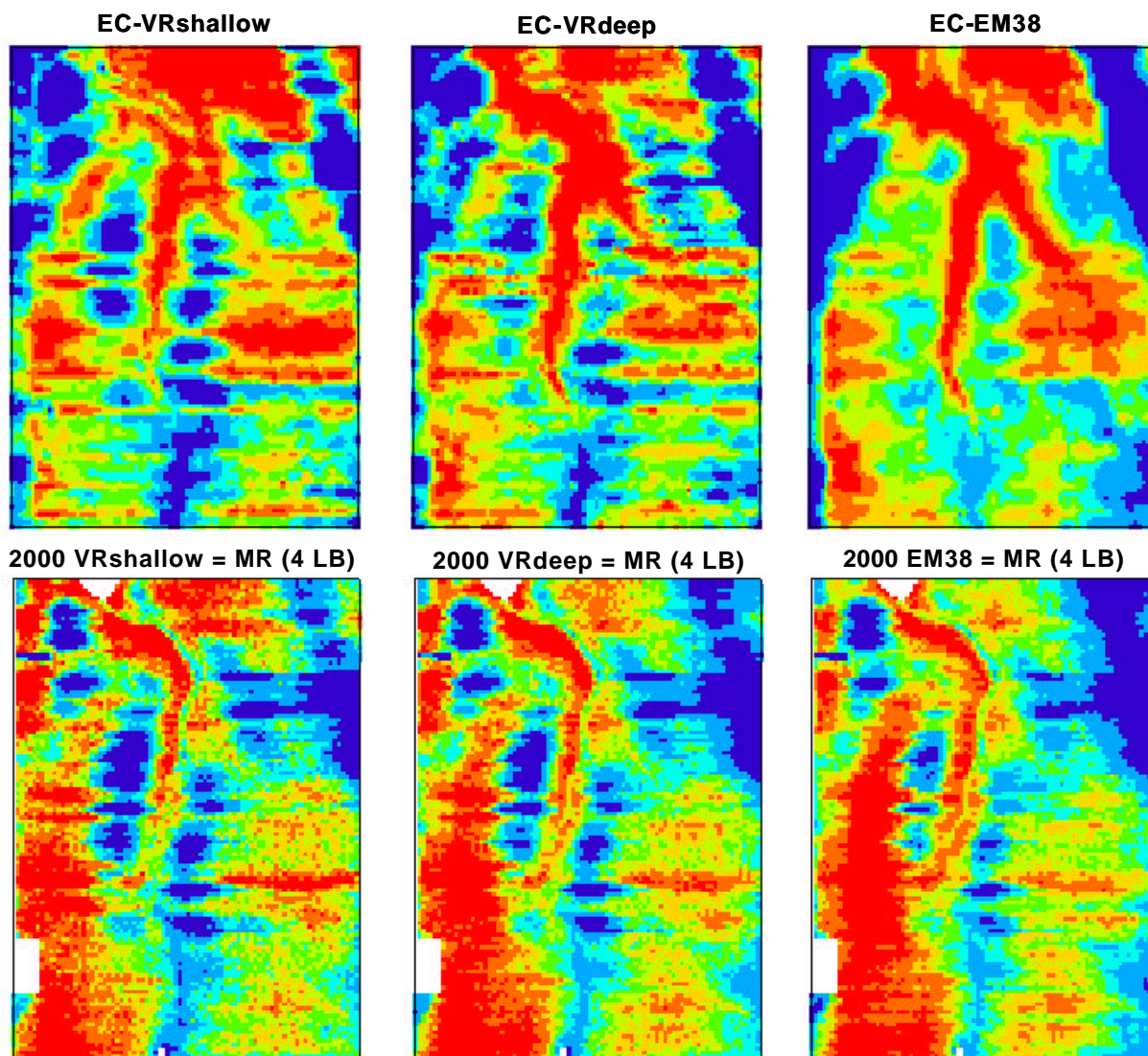


Figure 5. Soil EC maps by EM38 and Veris (top) and estimated EC maps (bottom) from MR (multiple regression) models using 4 Landsat-like bands.

### Principal Component Analysis

PCA has been used for dimensionality reduction of multispectral and hyperspectral images in pattern recognition applications and for creating an optimal set of spectral information from a large number of bands. Five PCs derived from the 120 HSI bands were correlated with soil EC<sub>a</sub> and fertility data (Table 2) because five PCs explained the vast majority of variance for the soil properties (>98%). The bare soil image from 2000 (dry soil) generally showed higher correlations to soil EC<sub>a</sub> and soil chemical properties than that of 2001 (wet soil). The highest correlations to soil EC<sub>a</sub> were found between PC 1 and EM38 and Veris deep readings in the 2000 image, and between PC 3 and EM38 and Veris deep readings in the 2001 image. The highest correlations to soil chemical properties were found between PC 2 and pH, OM, Mg, K, and CEC, and between PC 4 and pH, Mg, K, and CEC in the 2000 image. PC 1, which had the most variance of spectral signature, did not represent the soil chemical properties very well. Instead, PC 2 and PC 4 explained variability well for CEC, Mg, OM, K, and pH. Within-field soil fertility variability maps were made using PC 2 and PC 4 of the 2000 image (Figure 7). It seems clear that both approaches, using MR on Landsat-like bands, and PCA, have the capability to reduce the volume of HSI data and show potential for developing relationships with soil property variability.

#### ESTIMATING WITHIN-FIELD VARIATIONS IN SOIL PROPERTIES FROM AIRBORNE HYPERSPPECTRAL IMAGES

Table 1. SMLR models using 120 HSI bands and MR models using 4 Landsat-like bands (LBs) for estimating soil electrical conductivity and soil chemical properties from image data.

Dependent Variables	April 2000			May 2001		
	MR model for all LBs	SMLR model for all HSI bands		MR model for all LBs	SMLR model for all HSI bands	
		Full model	Conservative model		Full model	Conservative model
(n = 9588)	----- R <sup>2</sup> -----					
EC-EM38	0.33 <sup>***</sup>	0.56 <sup>***</sup> (62 <sup>1)</sup> )	0.54 <sup>***</sup> ( 9)	0.12 <sup>***</sup>	0.43 <sup>***</sup> (75)	0.41 <sup>***</sup> (25)
EC-VRsh	0.37 <sup>***</sup>	0.55 <sup>***</sup> (66)	0.52 <sup>***</sup> (16)	0.19 <sup>***</sup>	0.37 <sup>***</sup> (76)	0.35 <sup>***</sup> (34)
EC-VRdeep	0.36 <sup>***</sup>	0.50 <sup>***</sup> (58)	0.48 <sup>***</sup> (12)	0.18 <sup>***</sup>	0.36 <sup>***</sup> (68)	0.34 <sup>***</sup> (26)
(n = 335)	-----					
pH <sup>2)</sup>	0.49 <sup>***</sup>	0.68 <sup>***</sup> (35)	0.64 <sup>***</sup> (24)	0.31 <sup>***</sup>	0.66 <sup>***</sup> (40)	0.63 <sup>***</sup> (31)
Mg <sup>2)</sup>	0.48 <sup>***</sup>	0.67 <sup>***</sup> (26)	0.64 <sup>***</sup> (17)	0.30 <sup>***</sup>	- <sup>2)</sup>	-
CEC <sup>2)</sup>	0.44 <sup>***</sup>	0.66 <sup>***</sup> (32)	0.63 <sup>***</sup> (22)	0.25 <sup>***</sup>	-	-
K <sup>2)</sup>	0.36 <sup>***</sup>	0.59 <sup>***</sup> (24)	0.56 <sup>***</sup> (17)	0.21 <sup>***</sup>	-	-
OM <sup>2)</sup>	0.34 <sup>***</sup>	0.55 <sup>***</sup> (32)	0.52 <sup>***</sup> (25)	0.17 <sup>***</sup>	0.46 <sup>***</sup> (23)	0.44 <sup>***</sup> (19)
Ca <sup>2)</sup>	0.24 <sup>***</sup>	0.55 <sup>***</sup> (28)	0.52 <sup>***</sup> (21)	0.09 <sup>***</sup>	-	-
P <sup>2)</sup>	0.17 <sup>***</sup>	0.39 <sup>***</sup> (25)	0.37 <sup>***</sup> (22)	0.17 <sup>***</sup>	-	-

<sup>1)</sup> no. of wavelengths included <sup>2)</sup> no variable met the 0.15 significance level

Table 2. Relationship between soil EC readings and fertility, and HSI-derived principal components.

Variable	Year		PC1		PC2		PC3		PC4		PC5	
	R <sup>2</sup> of MR for all PCs		2000	2001	2000	2001	2000	2001	2000	2001	2000	2001
(n = 9588)	----- r -----											
EC-EM38	0.41 <sup>***</sup>	0.23 <sup>***</sup>	-0.49 <sup>***</sup>	-0.22 <sup>***</sup>	-0.05 <sup>***</sup>	-0.12 <sup>***</sup>	0.27 <sup>***</sup>	0.30 <sup>***</sup>	-0.03 <sup>**</sup>	0.07 <sup>***</sup>	-0.02 <sup>*</sup>	0.21 <sup>***</sup>
EC-VRsh	0.19 <sup>***</sup>	0.02 <sup>***</sup>	-0.30 <sup>***</sup>	-0.07 <sup>***</sup>	-0.02 <sup>*</sup>	-0.06 <sup>***</sup>	-0.02	0.06 <sup>***</sup>	-0.05 <sup>***</sup>	0.05 <sup>***</sup>	-0.02	-0.03 <sup>**</sup>
EC-VRdeep	0.31 <sup>***</sup>	0.12 <sup>***</sup>	-0.41 <sup>***</sup>	-0.13 <sup>***</sup>	-0.02	-0.11 <sup>***</sup>	0.11 <sup>***</sup>	0.24 <sup>***</sup>	-0.06 <sup>***</sup>	0.06 <sup>***</sup>	0.04 <sup>***</sup>	0.03 <sup>**</sup>
(n = 335)	-----											
pH	0.39 <sup>***</sup>	0.28 <sup>***</sup>	0.05	0.20 <sup>***</sup>	0.49 <sup>***</sup>	-0.06	0.11 <sup>*</sup>	-0.29 <sup>***</sup>	0.46 <sup>***</sup>	0.23 <sup>***</sup>	0.18 <sup>**</sup>	0.15 <sup>**</sup>
Mg	0.49 <sup>***</sup>	0.21 <sup>***</sup>	-0.32 <sup>***</sup>	-0.39 <sup>***</sup>	-0.46 <sup>***</sup>	-0.01	-0.10	0.12 <sup>*</sup>	-0.39 <sup>***</sup>	-0.10	-0.38 <sup>***</sup>	-0.10
CEC	0.41 <sup>***</sup>	0.14 <sup>***</sup>	-0.18 <sup>**</sup>	-0.27 <sup>***</sup>	-0.47 <sup>***</sup>	0.08	-0.14 <sup>*</sup>	0.03	-0.40 <sup>***</sup>	-0.15 <sup>***</sup>	-0.38 <sup>***</sup>	-0.10
K	0.37 <sup>***</sup>	0.06 <sup>***</sup>	-0.04	-0.17 <sup>**</sup>	-0.42 <sup>***</sup>	0.11 <sup>*</sup>	-0.02	-0.01	-0.33 <sup>***</sup>	0.02	-0.36 <sup>***</sup>	-0.08
OM	0.34 <sup>***</sup>	0.13 <sup>***</sup>	-0.06	-0.25 <sup>***</sup>	-0.45 <sup>***</sup>	0.16 <sup>**</sup>	-0.15 <sup>**</sup>	-0.08	-0.21 <sup>***</sup>	-0.03	-0.38 <sup>***</sup>	-0.05
Ca	0.12 <sup>***</sup>	0.07 <sup>***</sup>	-0.07	-0.06	-0.13 <sup>*</sup>	0.03	-0.08	-0.23 <sup>***</sup>	-0.09	0.01	-0.26 <sup>***</sup>	-0.01
P	0.18 <sup>***</sup>	0.19 <sup>***</sup>	0.07	-0.06	0.14 <sup>**</sup>	0.25 <sup>***</sup>	0.12 <sup>*</sup>	-0.31 <sup>***</sup>	0.45 <sup>***</sup>	0.25 <sup>***</sup>	-0.05	0.11 <sup>*</sup>

\* = 0.05 > p > 0.01, \*\* = 0.01 > p > 0.001, \*\*\* = p < 0.001

**ESTIMATING WITHIN-FIELD VARIATIONS IN SOIL PROPERTIES FROM AIRBORNE  
HYPERSPERTRAL IMAGES**

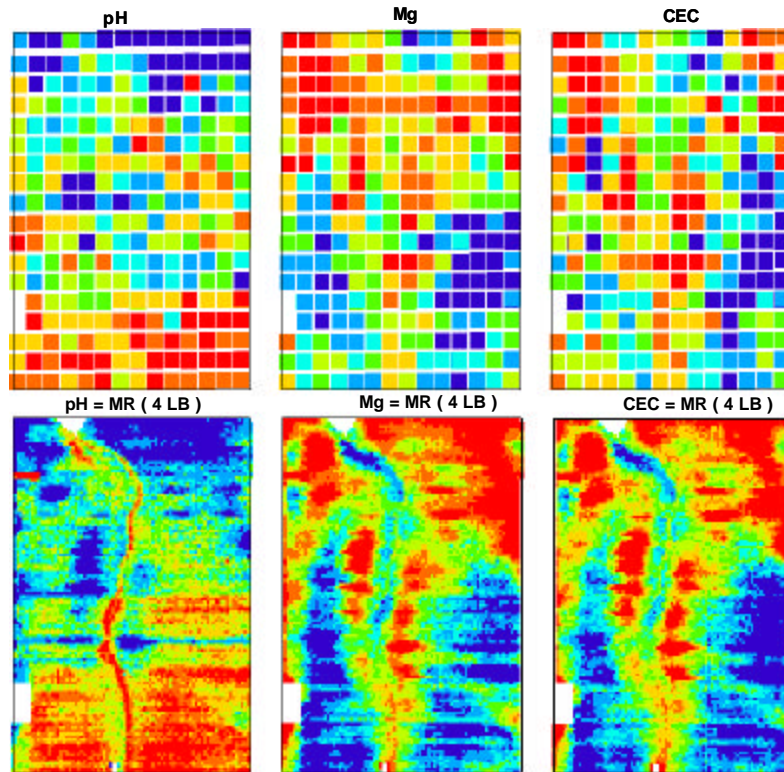


Figure 6. Maps of soil fertility from grid sampling (top) and estimated soil fertility maps from 4 Landsat-like bands (bottom) as derived from the 2000 bare soil image.

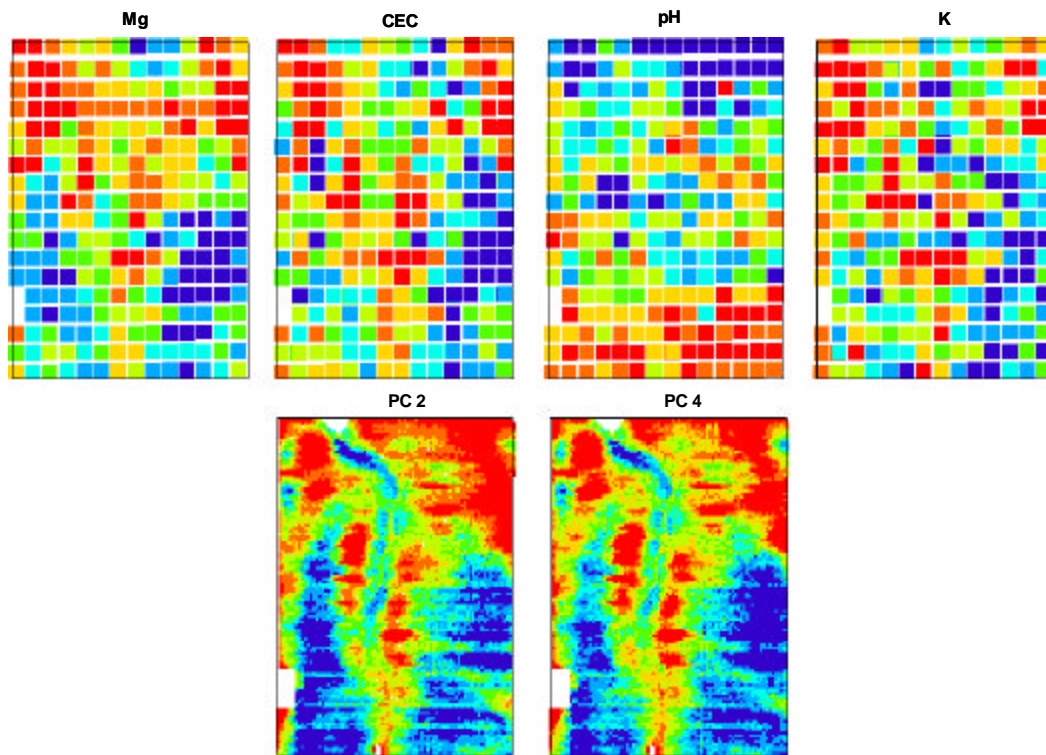


Figure 7. Soil fertility maps by grid soil sampling (top) and second and fourth principal component images (bottom) as derived from the 2000 bare soil image.

**ESTIMATING WITHIN-FIELD VARIATIONS IN SOIL PROPERTIES FROM AIRBORNE  
HYPER SPECTRAL IMAGES**

An important question raised through data analysis for both years' HSI was "why did the results differ between the two years?". Several factors which may have played a part were soil moisture conditions, image quality (mainly geometric distortion), different atmospheric conditions during image acquisition, and sun positioning.

Soil moisture conditions were significantly different between the two images. Spectral reflectance of the wet soil was lower, had a narrower range and had more deviation from the trend line. Soil moisture measurement and/or modeling during bare soil image acquisition may be necessary to better understand relationships between HSI and soil properties.

A number of potential error sources may have affected the results. Atmospheric models may need to be applied to compensate for atmospheric conditions and sun elevation. Sun positioning may also affect reflectance because of micro-relief in the field and different topographic aspects, and sun angle correction should be considered. The 2001 image was taken on May 9, ten days after planting (76 cm row spacing). Corn had emerged in the field and was approximately 5 cm tall, which could have slightly affected the soil spectral profile, though the effects should have been minor since 5 m-resolution pixels were selected for this analysis.

Noise reduction by image degradation worked since it improved the relationship between image data and ground sensed data as compared to previous results on part of this data without noise reduction (Hong *et al.*, 2001). Especially for airborne images, quality control in terms of signal to noise improvement is an important pre-processing step for image analysis. A homogeneous area method was used for this study. Other methods could be used to characterize signal to noise ratio such as the local means and local variances method and the geostatistical method (Van Der Meer *et al.*, 2001).

## CONCLUSIONS

Several statistical methods – simple correlation, MR, and PCA – were successfully used to relate within-field soil information with HSI and Landsat-like bands. HSI signatures of bare soil taken in April 2000 and May 2001 were correlated with soil EC<sub>a</sub> and soil chemical properties. Blue wavelengths in the visible region, Landsat-like band 1, and PC 2 and PC 4 of the HSI data were informative for estimating soil properties. SMLR models using HSI showed higher R<sup>2</sup> values than did MR models with Landsat-like bands, which demonstrates the value of HSI. But Landsat-like images were still quite good, and may be more acceptable for practical application, considering data volume, efficiency and overfitting concerns. PC maps using PC 2 and PC 4 also showed good relationships with soil pH, Mg, and CEC. While the soil data set did not include texture measurements we have found in other studies on claypan soil that CEC and texture is highly correlated (data unpublished). Therefore, it is reasonable to assert that reflectance variation for this field is largely a function of surface texture properties, such as noted by others (Barnes and Baker, 2000; Thomasson *et al.*, 2001). Both approaches, creating Landsat-like bands and PCA, reduced the volume of HSI data and showed potential for developing relationships with soil property variability.

Using a conservative SMLR model could reduce the chance of overfitting the data as compared to a full SMLR model. Estimated soil property maps from remote sensing described the spatial pattern of ground-sensed soil EC<sub>a</sub> and grid-sampled fertility. Many factors, mineral composition, moisture, organic matter, texture, and the like, are involved in spectral reflectance of soil. Clearly, soil moisture modeling will need further study, especially on Missouri claypan soils. However, HSI analysis appears promising for quantifying soil property variability.

## ACKNOWLEDGMENT AND DISCLAIMER

We thank the following for financial support or assistance enabling this research: North Central Soybean Research Program, United Soybean Board, Spectral Visions, NASA Scientific Data Purchase Program and USDA-CSREES Special Water Quality Grants Program. Mention of trade names or commercial products is solely for the purpose of providing specific information and does not imply recommendation or endorsement by the United States Department of Agriculture or its cooperators.

## REFERENCES

Baret F. and G. Guyot. (1991). Potentials and limits of vegetation indices for LAI and APAR assessment. *Remote Sens. Environ.*, 35:161-173.

### ESTIMATING WITHIN-FIELD VARIATIONS IN SOIL PROPERTIES FROM AIRBORNE HYPERSPETRAL IMAGES

- Barnes, E. M. and M. G. Baker. (2000). Multispectral data for mapping soil texture: Possibilities and limitations. *Applied Engineering in Agriculture*, 16(6):731-741.
- Bowers, S. A. and R. J. Hanks. (1965). Reflection of radiant energy from soil. *Soil Science*, 100:130-138.
- Baumgardner, M. F., L. F. Silva, L. L. Biehl, and E. R. Stoner. (1985). Reflectance properties of soils. *Advances in Agronomy*, 38:1-44.
- Brown, J. R. and R. R. Rodriguez. (1983). *Soil testing in Missouri: a guide for conducting soil tests in Missouri*. Extension Circular 923. Univ. of Missouri Extension Division, Columbia, Missouri.
- ERDAS Inc. (1997). *ERDAS Field Guide*, 4<sup>th</sup> Edition, ERDAS Inc. pp. 158-159, 225.
- Forghani A. (2000). Geometric registration of aerial photography using three image correction, In: *Proc. 2<sup>nd</sup> Intl. Conf. on Geospatial Information in Agriculture and Forestry*, Lake Buena Vista, FL, p. II-531-538 January 2000. Veridian, Arlington, VA.
- Goetz, A., G. Vane, J. E. Solomon, and B. N. Rock. (1985). Imaging spectrometry for earth remote sensing. *Science*, 228(4704):1147-1153.
- Hong, S. Y., K. A. Sudduth, N. R. Kitchen, H. L. Palm, and W. J. Wiebold. (2001). Using hyperspectral remote sensing data to quantify within-field spatial variability. CD-ROM. In: *Proc. 3<sup>rd</sup> Intl. Conf. on Geospatial Information in Agriculture and Forestry*, Denver, CO, 5-7 November 2001. Veridian, Arlington, VA.
- Huete, A. R. D. F. Post, and R. D. Jackson. (1984). Soil spectral effect on 4-space vegetation discrimination. *Remote Sens. Environ.* 15:155-165.
- Jensen, J. R. (2000). *Remote sensing of the environment; An earth resource perspective*, Prentice Hall, Upper Saddle River, New Jersey, p. 42, 227, 347.
- Karmanov, I. I. and V. A. Rozhkov. (1972). Experimental determination of quantitative relationships between the color characteristics of soils and soil constituents. *Soviet Soil Science*, 4(6):666-674.
- Kitchen, N. R., K. A. Sudduth, and S. T. Drummond. (1999). Soil electrical conductivity as a crop productivity measure for claypan soils. *J. Prod. Agric.*, 12:607-617.
- Mao, C. (2000). Hyperspectral focal plane scanning – An innovative approach to airborne and laboratory pushbroom hyperspectral imaging. In: *Proc. 2<sup>nd</sup> Intl. Conf. on Geospatial Information in Agriculture and Forestry*, Lake Buena Vista, FL, p. I-424-428 January 2000. Veridian, Arlington, VA.
- McNeill, J. D. (1980). Rapid, accurate mapping of soil salinity by electromagnetic ground conductivity meters. In: *Advances in Measurement of Soil Physical Properties: Bringing Theory Into Practice. Spec. Publ. 30, SSSA, Madison, WI*, pp. 209-229.
- Moran, M. S. (2000). Image-based remote sensing for agricultural management – Perspectives of image providers, research scientists and users. In: *Proc. 2<sup>nd</sup> Intl. Conf. on Geospatial Information in Agriculture and Forestry*, Lake Buena Vista, FL, p. I-23-30 January 2000. Veridian, Arlington, VA.
- Mulla, D. J., A. C. Sekey, and M. Beatty. (2000). Evaluation of remote sensing and targeted soil sampling for variable rate application of lime. CD-ROM. In: P.C. Robert *et al.* (ed.) *Proc. 5<sup>th</sup> Intl. Conf. on Precision Agriculture*, Minn., MN, Jul. 16-19, 2000. ASA, CSSA, and SSSA, Madison, WI.
- Obukhov, A. I. and D. S. Orlov. (1964). Spectral reflectivity of the major soil groups and possibility of using diffuse reflection in soil investigations. *Soviet Soil Science*, 2(2):174-184.
- Orlov, D. S. (1966). Quantitative patterns of light reflection by soils I. Influence of particle (aggregate) size. *Soviet Soil Science*, 13:1495-1498.
- Sudduth, K. A. and J. W. Hummel. (1991). Evaluation of reflectance methods for soil organic matter sensing. *Trans. ASAE*, 34(4):1900-1909.
- Sudduth, K. A., N. R. Kitchen, and S. T. Drummond. (1998). Soil conductivity sensing on claypan soils: comparison of electromagnetic induction and direct methods. In: *Proc. 4<sup>th</sup> Intl. Conf. on Precision Agriculture*, St. Paul, MN, p. 979-990 July 1998. ASA, CSSA, and SSSA, Madison, WI.
- Sudduth, K. A., S. T. Drummond, and N.R. Kitchen. (2001). Accuracy issues in electromagnetic induction sensing of soil electrical conductivity for precision agriculture. *Comp. and Electronics in Agric.*, 31: 239-264.
- Sudduth, K. A., N. R. Kitchen, G. A. Bollero, and D. G. Bullock. (2002). Comparison of electromagnetic induction and direct sensing of soil electrical conductivity. *Agron. J.* (in press)
- Thomasson, J. A., R. Sui, M. S. Cox, and A. Al-Rajehy. (2001). Soil reflectance sensing for determining soil properties in precision agriculture. *Trans. ASAE*, 44(6):1445-1453.
- Yao, H., A. Tian, and N. Noguchi. (2001). Hyperspectral imaging system optimization and image processing. In: *2001 ASAE Annual Intl. Meeting papers*, Paper no. 0.1-1105. Sacramento, CA, July 2001. ASAE, St. Joseph, MI
- Van der Meer, F. D. S. M. de Jong, and W. Baker. (2001). Imaging spectrometry: Basic analytical techniques. In: F. D. Van der Meer and S. M. de Jong. (ed.) *Imaging spectrometry*, 2000. Kluwer Academic Publishers, Boston, pp. 35-37.

## **ESTIMATING WITHIN-FIELD VARIATIONS IN SOIL PROPERTIES FROM AIRBORNE HYPERSPECTRAL IMAGES**